PHYSICAL REVIEW D **90,** 054025 (2014)

Non-Abelian bremsstrahlung and azimuthal asymmetries in high energy $p + A$ reactions

M. Gyulassy,[1,2,*] P. Levai,[1] I. Vitev,[3] and T. S. Biró[1]

[1]*MTA Wigner Research Centre for Physics, RMI, Budapest, Hungary*
[2]*Department of Physics, Columbia University, New York, New York 10027, USA*
[3]*Theoretical Division, Los Alamos National Laboratory, Los Alamos, New Mexico 87545, USA*
(Received 22 July 2014; published 25 September 2014)

We apply the GLV reaction operator solution to the Vitev-Gunion-Bertsch (VGB) boundary conditions to compute to all orders in nuclear opacity the non-Abelian gluon bremsstrahlung of event-by-event fluctuating beam jets in nuclear collisions. We evaluate analytically azimuthal Fourier moments of single gluon, $v_n^M\{1\}$, and even numbered 2ℓ gluon distribution, $v_n^M\{2\ell\}$, inclusive distributions in high-energy $p + A$ reactions as a function of harmonic n, target recoil cluster number, M, and gluon number, 2ℓ, at the RHIC and LHC. Multiple resolved clusters of recoiling target beam jets together with the projectile beam jet form color scintillation antenna (CSA) arrays that lead to characteristic boost-noninvariant trapezoidal rapidity distributions in asymmetric $B + A$ nuclear collisions. The scaling of the intrinsically azimuthally anisotropic and long range in η nature of the non-Abelian bremsstrahlung leads to v_n moments that are similar to results from hydrodynamic models, but due entirely to non-Abelian wave interference phenomena sourced by the fluctuating CSA. Our analytic nonflow solutions are similar to recent numerical saturation model predictions but differ by predicting a simple power-law hierarchy of both even and odd v_n without invoking k_T factorization. A test of the CSA mechanism is the predicted nearly linear η rapidity dependence of the $v_n(k_T, \eta)$. Non-Abelian beam jet bremsstrahlung may, thus, provide a simple analytic solution to the beam energy scan puzzle of the near $\sqrt{s}$ independence of $v_n(p_T)$ moments observed down to 10 AGeV, where large-x valence-quark beam jets dominate inelastic dynamics. Recoil bremsstrahlung from multiple independent CSA clusters could also provide a partial explanation for the unexpected similarity of v_n in $p(D) + A$ and noncentral $A + A$ at the same $dN/d\eta$ multiplicity as observed at the RHIC and LHC.

DOI: 10.1103/PhysRevD.90.054025 PACS numbers: 24.85.+p, 12.38.Cy, 25.75.-q

I. INTRODUCTION

An unexpected discovery at RHIC/BNL in $D + \mathrm{Au}$ reactions at $\sqrt{s} = 200$ AGeV [1] and at LHC/CERN in $\sqrt{s} = 5.02$ ATeV $p + \mathrm{Pb}$ reactions [2–4] is the large magnitude of midrapidity azimuthal anisotropy moments, $v_n(k_T, \eta = 0)$, that are remarkably similar to those observed previously in noncentral $\mathrm{Au} + \mathrm{Au}$ [5–7] and $\mathrm{Pb} + \mathrm{Pb}$ [8–12] reactions. See preliminary $p + \mathrm{Pb}$ data in Fig. 1, taken from ATLAS Ref. [13] Fig. 24, that also shows a large rapidity-even dipole v_1 harmonic [14].

In addition, the beam energy scan (BES) at RHIC [15] revealed a near $\sqrt{s}$ independence from 8 AGeV to 2.76 ATeV of the v_n in $A + A$ at fixed centrality that was also unexpected.

In high-energy $A + A$, the v_n moments have been interpreted as possible evidence for the near "perfect fluidity" of the strongly-coupled quark-gluon plasmas (sQGP) produced in such reactions [16–20]. However, the recent observation of similar v_n in much smaller $p(D) + A$ systems and, also, the near beam energy independence of the moments observed in the beam energy scan (BES) [15] from 7.7 AGeV to 2.76 ATeV in $A + A$ have posed a problem for the perfect fluid interpretation, because near inviscid hydrodynamics is not expected to apply in space-time regions where the local temperature falls below the confinement temperature, $T(x, t) < T_c \sim 160$ MeV. In that hadron resonance gas (HRG) "corona" region, the viscosity-to-entropy ratio is predicted to grow rapidly with decreasing temperature [21], and the corona volume fraction must increase relative to the ever-shrinking volume of the perfect fluid "core" with $T > T_c$ when either the projectile atomic number A and size $A^{1/3}$ fm or the center-of-mass (CM) energy $\sqrt{s}$ decreases.

While hydrodynamic equations have been shown to be sufficient to describe $p(D) + A$ data with particular assumptions about initial and freeze-out conditions [22,23], its necessity as a unique interpretation of the data is not guaranteed. This point was underlined recently using a specific initial-state saturation model [24] that was shown to be able to fit $p(D) + A$ correlation data on even v_n moments without final-state interactions.

That saturation model has also been used [19] to specify initial conditions for perfect fluid hydrodynamics in $A + A$. However, in $p + A$ such initial conditions for hydrodynamics are not as well controlled, because the gluon

*gyulassy@phys.columbia.edu

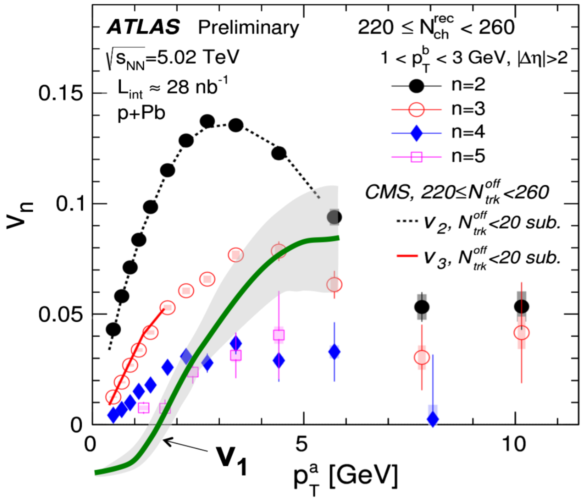

FIG. 1 (color online). $v_n(p_T)$ with $n = 2$ to 5 obtained for $|\Delta\eta| > 2$ and the p_T range of 1–3 GeV. An overlay sketch of preliminary rapidity-even v_1 data shown at QM14 [14] is also indicated by a dark green curve. The error bars and shaded boxes represent the statistical and systematic uncertainties, respectively. ATLAS $v_2(v_3)$ data in the $220 < N_{ch}^{rec} < 260$ range are compared to the CMS data [2] obtained by subtracting the peripheral events (the number of offline tracks $N_{off}^{trk} < 20$), shown by the dashed (solid) curves. Reproduced from ATLAS Ref. [13] $p + \mathrm{Pb}$ Fig. 24.

saturation scale, $Q_s(x, A = 1) < 1$ GeV, is small, and its fluctuations in the transverse plane on subnucleon scales are not reliably predicted.

The near independence of v_n moments on beam energy observed in BES [15] at RHIC from 7.7 AGeV to 2760 AGeV pose further serious challenges to the uniqueness of the perfect-fluid interpretations of the data because of previous predictions [25] for systematic reduction of the moments due to the increasing HRG corona. Those predictions appeared to be confirmed by SPS $\sqrt{s} =$ 17 AGeV data [26]. The most recent BES measurements, however, appear to contradict the diluting role of the HRG corona. The HRG corona fraction should dilute perfect-fluid QGP core flow signatures at lower energies unless additional dynamical mechanisms, possibly associated with increasing baryon density, accidentally conspire to compensate for the growing HRG corona fraction. Such a combination of canceling effects with $\sqrt{s}$ was demonstrated to be possible using a specific hybrid hydro + URQMD model [27] or three fluid models [28]. While such hybrid models are *sufficient* to explain the BES independence of v_2 data in $A + A$, the *necessity* and, hence, uniqueness of such hybrid descriptions are not guaranteed.

The BES [15] data also a pose a challenge to the color glass condensate (CGC) gluon saturation model [29] used to specify initial conditions for hydrodynamic flow predictions in $A + A$. This is because Q_s^2 is predicted to decrease with $\log(s)$, and thus gluon-saturation-dominated high-energy gluon fusion models of initial-state dynamics should switch over into valence-quark-diquark-dominated inelastic dynamics when partons with fractional energy $x > 0.01$ play the dominant role. At RHIC and lower energies, valence quark and diquark QCD string phenomenology based on the LUND model [30] and its $B + A$ generalization to nuclear collision via the HIJING model [31] can smoothly interpolate between AGS and RHIC energies. Such a multiple-beam-jet-based approach to $B + A$ naturally accounts, for example, for the striking long-range triangular, boost-noninvariant form of $(dN_{pA}/d\eta)/(dN_{pp}/d\eta)$ nuclear enhancement of the final hadron rapidity density in $p(D) + A$ observed at all CM energies up to LHC [32]. By including multiple mini- and hard-jet production, it can account for the $\sqrt{s}$ growth of $dN_{B+A}/d\eta$; though at top $\sqrt{s} = 200$ AGeV RHIC and at LHC energies, there is strong evidence for the onset of gluon saturation [33] that limits $2 \to 2$ minijet processes to $p_T > Q_s(x, A) \propto A^{1/3}/x^\lambda$ that grows with A and $1/x = \sqrt{s}/(p_T e^\eta)$.

The importance of multiple beam jets with rapidity kinematics controlled by valence quarks and diquarks was first proposed within the Brodsky-Gunion-Kuhn (BGK) model [34], which is reproduced also in the HIJING [35] model. The trapezoidal boost-noninvariant dependence of the local density, $dN/d\eta d^2\mathbf{x}$, predicted in Ref. [35] as a function of the transverse coordinate $\mathbf{x}$ even in symmetric $A + A$, may also play an important role in the triangular long-range η dependence of $v_2(\eta, \sqrt{s})$ as observed in Au + Au by PHOBOS [36].

In this paper we explore the possibility that a dynamical source, that could partially account for the above puzzling azimuthal moment systematics, may be traced to a basic perturbative QCD (pQCD) feature. The pQCD based model here extends the opacity $\chi = 1$ Gunion-Bertsch [37] (GB) perturbative QCD bremsstrahlung used to model. $\pi + \pi \to g + X$ to all orders in opacity, $e^{-\chi} \sum_{n=1}^{\infty} \chi^n/n! \ldots$, Vitev-Gunion-Bertsch (VGB) multiple-interaction pQCD bremsstrahlung for applications to $B + A$ nuclear collisions. We show that VGB bremsstrahlung naturally leads on an event-by-event basis to a hierarchy of nontrivial azimuthal asymmetry moments similar to that observed in $p + A$ (see Fig. 1) and peripheral $A + A$ at fixed $dN/d\eta$ [9,11,12].

A particularly important feature of beam jet non-Abelian bremsstrahlung is that it automatically leads to long-range rapidity η "ridge" correlations and to azimuthal asymmetry harmonics from $n = 1, 2, 3, \ldots$. Conventional Lund-string beam jet models [30], as encoded, e.g., in HIJING, on the other hand, neglect recoil-induced moderate p_T color bremsstrahlung azimuthal asymmetries. From the pQCD perspective, beam jets are simply arrays of parallel color antennas that radiate due to multiple soft transverse momentum transfers $|\mathbf{q}_i| \sim 1$ GeV between participant projectile and $i = 1, \ldots, N_T(b)$ target nucleons. Many event generators include *ϕ-averaged* (azimuthally randomized) bremsstrahlung effects via $\sim\alpha_s/k_T^2$ up to the minijet scale $k_T < Q_s(x, A)$. In HIJING, the ARIADNE [38] code is used in conjunction with the nonperturbative Lund string fragmentation code JETSET [39] to incorporate this effect, while highly azimuthally asymmetric hard pQCD jets with $k_T > Q_s(x, A)$ are included via the PYTHIA [39]) code. In Ref. [30] it was emphasized that the high string tension of color strings reduces greatly the sensitivity of Lund string fragmentation to QCD bremsstrahlung and is an important infrared safety feature of that nonperturbative hadronization phenomenology.

In $p + A$ multiple collisions, however, the projectile accumulates multiple transverse momentum kicks (the Cronin effect) from scattering with cold nuclear participants [40,41] that enhances the bremsstrahlung mean square $\langle k_T^2 \rangle_{pA} \approx A^{1/3}\mu^2$ via random walk in the target frame. In the CGC approach, this $A^{1/3}$ growth is built into $Q_s^2(x, A)$ in the infinite momentum frame.

At the minijet scale, the underlying azimuthal asymmetry of non-Abelian bremsstrahlung will tend to focus gluons toward the azimuthal directions of exchanged momenta. At present, this basic azimuthal dependence is not taken into account in HIJING.

As we show below, there is a very important aspect to the multiple color antenna arrays in high-energy $p + A$ due to the longitudinal coherence of clusters of participant target beam jets separated by small transverse coordinates, too small to be resolved by the transverse momenta involved. While the total average number of Glauber participant nucleons that interact with a projectile at impact parameter $\mathbf{b}$ is determined by the area of the inelastic cross section $\sigma_{in}(s) \sim \text{few fm}^2$ as $N_T(\mathbf{b}) = \sigma_{in}(s) \int dz \rho_T(z, \mathbf{b})$, for moderate momentum transfers with $k_T \sim Q_s \sim 1$–2 GeV bremsstrahlung, the target participant antennas naturally group event-by-event into $M \leq N_T$ resolved clusters separated in the transverse plane by subnucleon distances $1/k_T \sim 0.2$ fm, similar to the CGC model [42] and in AdS/CFT shock modeling [43] of $p + A$, but here simply to the transverse resolution scale of multiple scattering recoil kinematics in the target frame versus the infinite-momentum frame.

This partial decoherence of the $N_T(b)$ participating target dipoles creates nonisotropic spatial distributions of color antennas that radiates according to the fluctuating spatial asymmetries from event to event. Each cluster is characterized by the number m_a of target participant dipole antennas that exchange coherently $Q_a^2 = m_a \mu^2$ with the projectile at a specific azimuthal angle ψ_a controlled by the transverse geometrical distribution of the clusters.

Each recoil cluster $a = 1, \ldots, M$ radiates coherently into a broad range of rapidities that appears in two particle correlations as a beam jet "ridge" component with $\mathbf{k}$ enhanced near $-\mathbf{Q}_a = -\sum_{i \in I_a} \mathbf{q}_i$. In addition, the projectile cluster radiates coherently into a broad range of rapidities but with transverse momenta $\mathbf{k}$ enhanced near $\mathbf{Q}_0 = (Q_0, \psi_0) = \sum_{a=1}^{M} \mathbf{Q}_a$. On an event-by-event basis, M and the color antenna geometry fluctuate, producing naturally $n = M + 1$ and other azimuthal harmonics in two-gluon $v_n = \langle \cos(n(\phi_1 - \phi_2)) \rangle$.

Our goal here is to estimate analytically the magnitude of the color bremsstrahlung source of pQCD dynamical azimuthal two-particle correlations and its dependence on n, k, M, N_T. We illustrate the results with specific analytic cluster geometric limits, including Z_n symmetric and Gaussian random CSA. We propose a future generalization of HIJING that could enable more realistic testing the influence of anisotropic VGB bremsstrahlung on the final hadron flavor-dependent azimuthal moments and competing minijet and hard-jet sources of anisotropies.

II. FIRST-ORDER IN OPACITY (GUNION-BERTSCH) BREMSSTRAHLUNG AND AZIMUTHAL ASYMMETRIES v_n

The above puzzles with BES [15], $D +$ Au at RHIC, and $p +$ Pb at LHC motivate us to consider an alternative: more basic, perturbative QCD sources of azimuthal asymmetries. The well-known non-Abelian bremsstrahlung Gunion-Bertsch (GB) formula [37] for the soft-gluon radiation single-inclusive distribution is

$$\frac{dN_g^1}{d\eta d^2\mathbf{k} d^2\mathbf{q}} = \frac{C_R \alpha_s}{\pi^2} \frac{\mu^2}{\pi(q^2 + \mu^2)^2} \frac{\mathbf{q}^2}{\mathbf{k}^2(\mathbf{k} - \mathbf{q})^2}, \qquad (1)$$

where we characterize the parton-scattering elastic cross section $d\sigma_0/d^2\mathbf{q} = \sigma_0 \mu^2/\pi(q^2 + \mu^2)^2$ off color-neutral target participants with a momentum transfer $\mathbf{q}$ in terms of a characteristic cold nuclear matter scale $\mu^2 \approx 0.12$ GeV^2 taken from fits to forward dihadron correlations in Refs. [44–46]. Here $q = |\mathbf{q}|$, and the produced gluon has rapidity η and transverse momentum $\mathbf{k}$ ($k = |\mathbf{k}|$) in the final state. It is obvious from Eq. (1) that non-Abelian gluon bremsstrahlung is preferentially emitted along two directions specified by the beam "$\hat{\mathbf{z}}$" axis and the transverse momentum transfer vector $\mathbf{q}$. The uniform rapidity-even $\eta \approx \log(xE/k)$ distribution associated with moderate $\mathbf{q}$ scattering is a unique feature of non-Abelian bremsstrahlung in the kinematic $k \ll xE \ll E$ range of interest associated with beam jets and is due to the triple gluon vertex. The uniform rapidity-even distribution is an especially important characteristic of non-Abelian radiation. The combination of the two leads to a uniform rapidity "ridge" in the direction of the momentum transfer $\mathbf{q}$ that fluctuates in both magnitude and direction from event to event but is measurable in two-or-higher-gluon correlation measurements. The rapidity-even ridge is, of course, kinematically limited to the $\eta \in [Y_T, Y_P]$ interval between the target and projectile rapidities. Independent but kinematically correlated multiple target and projectile beam jet bremsstrahlung sources can account for the triangle boost-noninvariant rapidity density observed in $p + A$.

For the scattering of color neutral dipoles considered in Ref. [37], the Rutherford perturbative α^2/q^4 distribution of momentum transfers was modeled by color-neutral form factors of the form $q^2(q^2+\mu^2)^{-1}$. For GB radiation, the $\mathbf{k}=\mathbf{q}$ singularity is also regulated by such a form factor. Therefore, the color neutralization scale μ^2 regulates the $(\mathbf{k}-\mathbf{q})^2$ singularity in Eq. (1) as well. The x and A dependence of that scale arises naturally in small-x models based the gluon saturation scale $Q_s(x,A)$ [29,42,47]. Our emphasis here, however, is to explore the general characteristics of semi-hard bremsstrahlung from the perturbative QCD perspectives that allow us to derive analytically many of the observed remarkably simple scaling relations between 2ℓ azimuthal harmonic cummulants, $v_n(2\ell)$, as a basic coherent-state semiclassical wave interference effect without invoking hydrodynamic local equilibrium assumptions.

The screened single inclusive GB perturbative gluon distribution is

$$\frac{dN_g^{(1)}}{d\eta d^2\mathbf{k}d^2\mathbf{q}} \equiv f(\eta,\mathbf{k},\mathbf{q}) = \frac{C_R\alpha_s}{\pi^2k^2}\frac{\mu^2q^2}{\pi(q^2+\mu^2)^2}\frac{P_\eta}{(\mathbf{k}-\mathbf{q})^2+\mu^2} \tag{2}$$

$$\equiv \frac{FP}{A-\cos(\phi-\psi)}, \tag{3}$$

where ϕ is the azimuthal angle of $\mathbf{k}$ and ψ is the azimuthal angle of $\mathbf{q}$, using the abbreviations

$$A \equiv A_{kq} \equiv (k^2+q^2+\mu^2)/(2kq) \geq 1, \tag{4}$$

$$F \equiv F_{kq} \equiv \frac{C_R\alpha_s}{\pi^2k^2}\frac{\mu^2q^2}{\pi(q^2+\mu^2)^2}\frac{1}{2kq}, \tag{5}$$

$$P \equiv P_\eta \equiv (1-e^{Y_T-\eta})^{n_f}(1-e^{\eta-Y_P})^{n_f}, \tag{6}$$

where we introduce a kinematic rapidity envelope factor P_η corresponding to approximately uniform rapidity dependence of the non-Abelian bremsstrahlung [37] regulated with $(1-|x_F|)^{n_f}$ kinematic spectator power counting [47,48]. Note that $n_f = 2n_{\rm spec}-1 \sim 4$ for gluon production from the scattering of two color-neutral dipoles in the large $|x_F| \to 1$ limit. The P_η rapidity envelopes can be used to build up multi-beam-jet boost-noninvariant triangular $dN_{pA}/d\eta$ as in the BGK [34] model and also to model the intrinsic boost-noninvariance of $dN_{AA}/d\eta d\mathbf{x}_\perp$ in even and symmetric $A+A$ collisions, as with HIJING [35].

The single-gluon azimuthal moments, $v_n = v_n\{1\}$ in cumulant notation, from a single GB color antenna defined by the momentum transfer $\mathbf{q}=(q,\psi)$ with azimuthal angle ψ are defined by

$$\begin{aligned} v_n^{\rm GB}(k,q,\psi)f_0(k,q) &= FP\int\frac{d\phi}{2\pi}\frac{\cos(n\phi)}{A-\cos(\phi-\psi)} \\ &= FP\mathrm{Re}\oint_{|z|=1}\frac{dz}{2\pi i}\frac{(-2e^{in\psi})z^n}{(z^2-2Az+1)} \\ &= FP\mathrm{Re}\frac{2(e^{i\psi}z_-)^n}{z_+-z_-}, \end{aligned} \tag{7}$$

where we defined $z \equiv \exp(i(\phi-\psi))$, so that $d\phi = -idz/z$ and $\cos(\phi-\psi) = (z+1/z)/2$. Note that there are two simple real poles $z_\pm = A \pm \sqrt{A^2-1}$. Since $A \geq 1$, only z_- contributes to the unit contour integral, resulting in the final analytic expression above. Note that the azimuthal averaged single-gluon-inclusive ($n=0$) bremsstrahlung distribution with $v_0 = 1$ is then

$$\begin{aligned} f_0 &= 2FP/(z_+-z_-) = F_{kq}P_\eta/(A_{kq}^2-1)^{1/2} \\ &\propto dN/d\eta dk^2dq^2. \end{aligned} \tag{8}$$

This has a linear divergence at $k=q$ in the $\mu=0$ limit in addition to the usual Abelian collinear $1/k^2$ divergence. The first is regulated by the color-neutral dipole form factor in the GB model.

The azimuthal Fourier moments are, however, finite in Eq. (7), even in the case of vanishing μ, and depend analytically on n and A via

$$v_1^{\rm GB}(k,q,\psi) = \cos[\psi](A_{kq}-\sqrt{A_{kq}^2-1}), \tag{9}$$

$$\lim_{\mu\to 0} v_1^{\rm GB}(k,q,0) = (k/q)\theta(q-k), \tag{10}$$

$$v_n^{\rm GB}(k,q,\psi) = \cos[n\psi](v_1^{\rm GB}(k,q,0))^n, \tag{11}$$

$$\lim_{\mu\to 0} v_n^{\rm GB}(k,q,0) = (k/q)^n\theta(q-k). \tag{12}$$

Note that in the $\mu=0$ limit, all $v_n \to 1$ reach unity at $k=q$ but vanish for $k>q$. For finite $\mu>0$, all moments maximize at $k^2 = k_*^2 = q^2+\mu^2$ with $v_n(k_*) = (\sqrt{(1+\mu^2/q^2)}-\mu/q)^n$. Figure 2 illustrates the magnitude of GB $v_n(k/\mu, q/\mu)$ moments as a function of k/μ for $n=1,\ldots,5$ and two different $q/\mu = 1, 3$.

Note the remarkable power-law scaling with n (for fixed $k,q.\psi$) of the azimuthal moments of gluon bremsstrahlung from a single GB color antenna:

$$[v_n^{\rm GB}(k,q,0)]^{1/n} = [v_m^{\rm GB}(k,q,0)]^{1/m}, \tag{13}$$

that is similar to the scaling observed by ALICE, CMS and ATLAS [4,8,11] at LHC, at least for the higher $n \geq 3$ moments dominated by purely geometric fluctuations. This scaling is, of course, not expected to hold perfectly for an ensemble averaged over q ratios of $\cos(n\Delta\phi)$ averaged dihadron-inclusive rates. One of our aims below is to test the survival of the above ideal scaling in Eq. (13) to ensemble averages in two-gluon-inclusive processes.

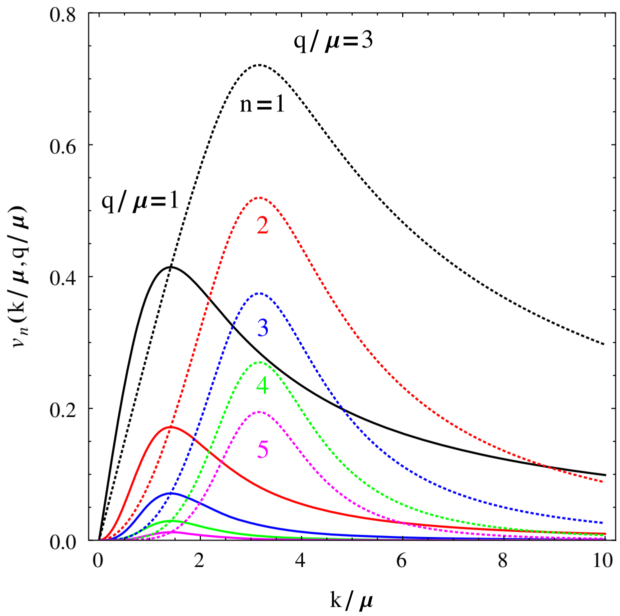

FIG. 2 (color online). Single GB beam jet bremsstrahlung azimuthal Fourier moments, $v_n^{\rm GB}(k,q)$ from Eq. (11), are shown versus k/μ for $n=1-5$ for $q/\mu=1(3)$ as solid (dashed) curves.

However, note that by rotation invariance, all harmonics $n>0$ vanish for *single*-inclusive GB antennas when averaged over the momentum transfer azimuthal angle ψ. We show below in Sec. V that the finite rms fluctuating harmonics of *two-particle*-inclusive $(\langle\cos(n\Delta\phi)\rangle)^{1/2}$ survive with similar magnitude and k dependence as in Figs. 2 and 3.

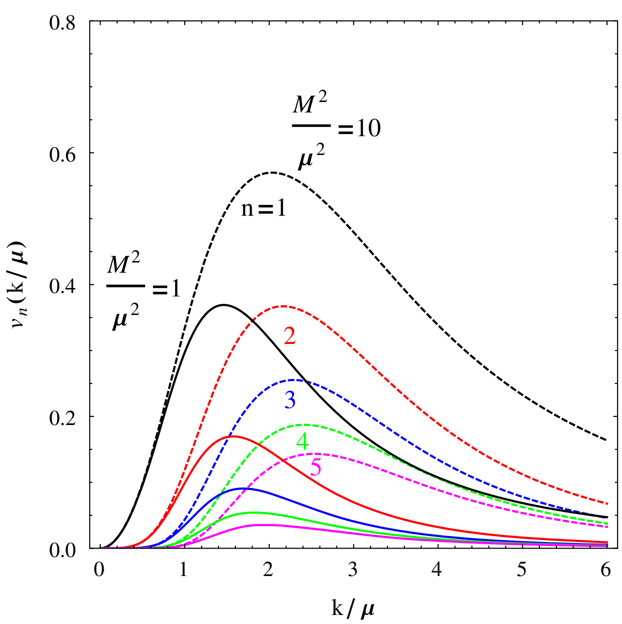

FIG. 3 (color online). Single GB beam jet bremsstrahlung azimuthal Fourier moments, $\langle v_n^{\rm GB}(k,q)\rangle_q$ averaged over q with $M^2/(q^2+M^2)^2$, are shown versus k/μ for $n=1-5$ for $(M/\mu)^2=1(10)$ as solid (dashed) curves.

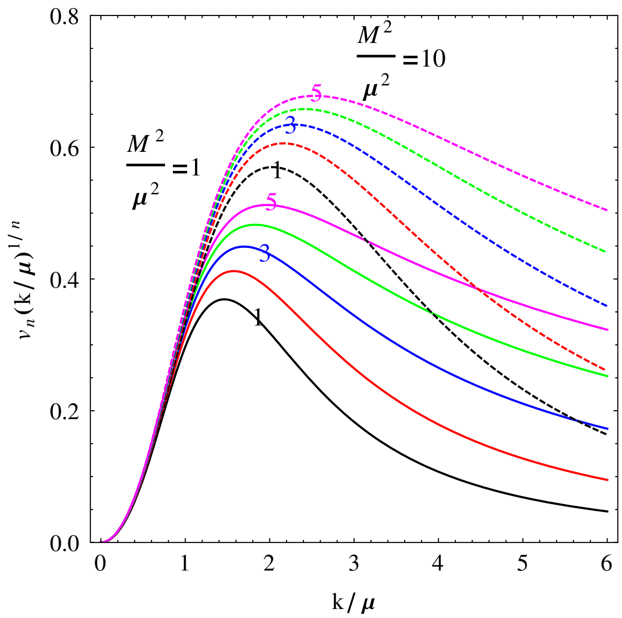

FIG. 4 (color online). The ideal $1/n$ power scaling of q averaged $\langle v_n^{\rm GB}(k,q)\rangle^{1/n}$ with $k\lesssim M$ [see Eq. (11)] breaks down at higher k, because in the $\mu=0$ limit of non-Abelian bremsstrahlung limits, $k\le q$ [see Eq. (12)].

In Fig. 4, we see that the simple fixed-q power-law scaling of Eqs. (11) and (13) holds for $k/M<1$ but gradually breaks down at higher $k>M$ when the ensemble is averaged over q^2 in $\langle f_n(k)\rangle$.

III. ALL ORDERS IN OPACITY VGB GENERALIZATION OF GUNION-BERTSCH RADIATION

A recursive reaction operator method was originally developed in GLV [49,50] to compute final-state multiple-collision-induced gluon bremsstrahlung and elastic collisional energy loss [40] to all orders in opacity for applications to jet quenching. Extensions of the method to final-state heavy-quark jet energy loss was given in Refs. [51,52].

Vitev further extended the reaction operator method to compute non-Abelian energy loss in cold nuclear matter in Ref. [53]. In addition to final-state (FS) bremsstrahlung, Vitev solved the cold matter initial-state (IS) bremsstrahlung problem to all orders in opacity, and also the generalization of the first-order in opacity Gunion-Bertsch [37] non-Abelian bremsstrahlung problem to all orders in opacity for the asymptotic $(t_0\to-\infty, t_f\to+\infty)$ boundary condition. We refer here to the Vitev all-order in opacity generalized GB radiation solution as VGB.

In Ref. [53], the VGB solution was regarded to be of mainly academic interest, since the focus there was on induced initial-state and final-state gluon bremsstrahlung associated with hard processes in $p+A$ [44–46]. In this paper, we focus entirely on the application of the VGB solution to low-to-moderate-transverse-momentum

$k <$ few GeV gluon radiation from multiple beam jets in the same spirit as in GB [37], where the aim was to understand the general qualitative characteristics of inelastic high-energy single-inclusive processes from a low-order perturbative QCD perspective.

Our aim here is to calculate azimuthal asymmetry moments, $v_n(\eta, \mathbf{k})$, arising from basic perturbative QCD bremsstrahlung effects in high-energy $p+A$ interactions. The physical picture approximates $p+A$ scattering as the scattering of an incoming color dipole at an impact parameter, $\mathbf{b}$, of high (positive) rapidity $Y_P \gg 1$ with $N_T^{\text{part}} \sim A^{1/3}$ nuclear target participant nucleons with high (negative) $Y_T \ll -1$ in the CM. The target participant dipoles at a fixed transverse coordinate $\mathbf{R}$ are separated by longitudinal separations $\Delta z_i = z_i - z_{i-1} \sim \text{fm}$ in the cold nucleus target rest frame. However, they act coherently when emitting gluons near midrapidity due to Lorentz contraction in the CM and the long formation time of gluons $\sim [2\cosh(\eta)]/k$ in the lab frame.

However, the target participants are distributed in the transverse direction by transverse separations $R_{ij} = |\mathbf{R}_i - \mathbf{R}_j| \lesssim \sqrt{\sigma_{in}/\pi} \sim \text{fm}$, which can be resolved for $k > 1$ GeV. This can lead to multiple incoherent groups or clusters of target participant nucleons that radiate coherently gluons with $|\eta| < 1$, $k > 1$ GeV gluons coherently. We propose in Sec. IV below a simple percolation model to estimate the partially coherent target recoil bremsstrahlung. However, we concentrate in this section on the coherent projectile bremsstrahlung contribution.

The complete VGB solution to all orders in opacity, $\chi \equiv \chi(\mathbf{b}) = \int dz \sigma_g(z) \rho(z, \mathbf{b})$, derived by Vitev in Ref. [53] is

$$\frac{dN^{\text{VBG}}}{d\eta d^2\mathbf{k}} = \sum_{n=1}^{\infty} \frac{dN_n^{\text{VBG}}}{d\eta d^2\mathbf{k}} = \frac{C_R \alpha_s}{\pi^2} \sum_{n=1}^{\infty} \left[\prod_{i=1}^{n} \int \frac{d\Delta z_i}{\lambda_g(z_i)}\right] \left[\prod_{j=1}^{n} \int d^2\mathbf{q}_j (v_j^2(\mathbf{q}_j) - \delta^2(\mathbf{q}_j))\right] \times \mathbf{B}_{21}^{b} \cdot \left[\mathbf{B}_{21}^{n} + 2\sum_{i=2}^{n} \mathbf{B}_{(i+1)i}^{n} \cos\left(\sum_{j=2}^{i} \omega_{jn} \Delta z_j\right)\right], \tag{14}$$

where the transverse vector "antenna" amplitudes $\mathbf{B}_{jk}^n$ are defined in terms of differences between "cascade" vector amplitudes $\mathbf{C}_{jn}$ as

$$\mathbf{B}_{jk}^n = \mathbf{C}_{jn} - \mathbf{C}_{kn}, \tag{15}$$

$$\mathbf{C}_{jn} = \frac{\mathbf{k} - \mathbf{q}_j - \cdots - \mathbf{q}_n}{(\mathbf{k} - \mathbf{q}_j - \cdots - \mathbf{q}_n)^2} = \frac{\mathbf{k} - \mathbf{Q}_{jn}}{(\mathbf{k} - \mathbf{Q}_{jn})^2}. \tag{16}$$

Indices j, k, n here keep track of combinations of nonvanishing momentum transfers $\mathbf{q}_i$ from direct versus virtual diagrams contributing at a given opacity order n of the opacity expansion. The partial summed momentum transfers are $\mathbf{Q}_{jn} = \sum_{i=j}^{n} \mathbf{q}_i$, being the singular directions of non-Abelian bremsstrahlung that also control the inverse formation times

$$\omega_{jn} = \frac{(\mathbf{k} - \mathbf{Q}_{jn})^2}{2E_g}. \tag{17}$$

Here $E_g = xE_P \ll E_P$ is the energy of the gluon in a frame where the energy of the proton projectile is assumed to be large, $E_P \gg m_n$.

There are two simple limits depending on the kinematic range of interest. In the coherent or factorization limit where $n\omega_{jn}\lambda_g \ll 1$, we can approximate all the cosines by unity. This is the limit we are interested in for our present applications to midrapidity multiparticle production not too close to projectile and target fragmentation regions, i.e., $Y_T + 1 < \eta < Y_P - 1$.

The target scattering centers are ordered in this VGB problem as $z_0 = -\infty < z_1 < \cdots < z_n < z_f = +\infty$ with $\Delta z_i = (z_i - z_{i-1})$ for $i \geq 2$. $\sigma_g(z)\rho(z, \mathbf{b})$ is the local inverse mean free path of a gluon with the nuclear target at position z impact parameter $\mathbf{b}$ in the target rest frame. The $v^2(\mathbf{q}_j) = \frac{d\sigma_{el}(z_j)}{d^2\mathbf{q}_j}$ denote normalized distributions of transverse momentum transfers at the scattering center z_j.

In the coherent scattering limit of relevance to near midrapidity radiation, and neglecting possible z dependence of the screening scale μ of the normalized distribution $v^2(\mathbf{q})$, we can write more explicitly at the impact parameter $\mathbf{b}$

$$\frac{dN_{\text{coh}}^{\text{VGB}}}{d\eta d^2\mathbf{k}} = \frac{C_R \alpha_s}{\pi^2} \sum_{n=1}^{\infty} \left[\prod_{i=1}^{n} \int d\Delta z_i \sigma_{el}(z_i) \rho(z_i, \mathbf{b})\right] \left[\prod_{j=1}^{n} \int d^2\mathbf{q}_j \left(\frac{1}{\sigma_{el}} \frac{d\sigma_{el}}{d^2\mathbf{q}_j} - \delta^2(\mathbf{q}_j)\right)\right] \times \left(\frac{\mathbf{k} - \mathbf{q}_2 - \cdots - \mathbf{q}_n}{(\mathbf{k} - \mathbf{q}_2 - \cdots - \mathbf{q}_n)^2} - \frac{\mathbf{k} - \mathbf{q}_1 - \cdots - \mathbf{q}_n}{(\mathbf{k} - \mathbf{q}_1 - \cdots - \mathbf{q}_n)^2}\right) \cdot \left[\left(\frac{\mathbf{k} - \mathbf{q}_2 - \cdots - \mathbf{q}_n}{(\mathbf{k} - \mathbf{q}_2 - \cdots - \mathbf{q}_n)^2} - \frac{\mathbf{k} - \mathbf{q}_1 - \cdots - \mathbf{q}_n}{(\mathbf{k} - \mathbf{q}_1 - \cdots - \mathbf{q}_n)^2}\right) + 2\sum_{i=2}^{n} \left(\frac{\mathbf{k} - \mathbf{q}_{i+1} - \cdots - \mathbf{q}_n}{(\mathbf{k} - \mathbf{q}_{i+1} - \cdots - \mathbf{q}_n)^2} - \frac{\mathbf{k} - \mathbf{q}_i - \cdots - \mathbf{q}_n}{(\mathbf{k} - \mathbf{q}_i - \cdots - \mathbf{q}_n)^2}\right)\right]. \tag{18}$$

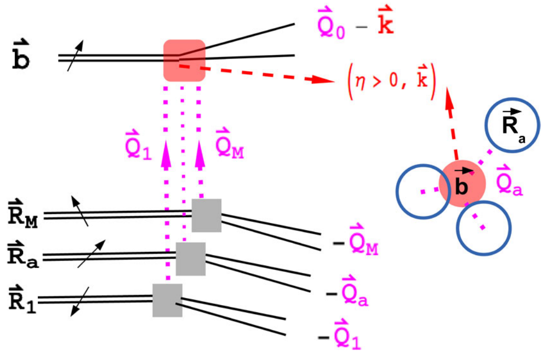

FIG. 5 (color online). Schematic diagram corresponding to coherent bremsstrahlung from the projectile dipole from Eqs. (19) and (20). At opacity order n, the azimuthal distribution is enhanced for transverse momenta $\mathbf{k}$ near the total accumulated momentum transfer $\mathbf{Q}_0 \equiv \mathbf{Q}_{1n} = \sum_a \mathbf{Q}_a$, where $a = 1, \ldots, M$ groups of recoiling target dipoles.

In order to extract the physical interpretation of the above compete but unwieldy expression, we derive in Appendix A the linked cluster theorem version of Eq. (18) to be

$$dN^{\mathrm{VGB}}_{\mathrm{coh}}(\mathbf{k}) = \sum_{n=1}^{\infty} \int d^2\mathbf{Q} P_n^{el}(\mathbf{Q}) dN^{\mathrm{GB}}(\mathbf{k}, \mathbf{Q}), \tag{19}$$

where $P_n^{el}(\mathbf{Q})$ is the probability density that, after n elastic scatterings, the cumulative total momentum transfer is $\mathbf{Q}$,

$$P_n^{el}(\mathbf{Q}) = \exp[-\chi] \frac{\chi^n}{n!} \int \left\{ \prod_{j=1}^{n} \frac{d^2\mathbf{q}_j}{\sigma_{el}} \frac{d\sigma_{el}}{d^2\mathbf{q}_j} \right\} \times \delta^2(\mathbf{Q} - (\mathbf{q}_1 + \cdots + \mathbf{q}_n)), \tag{20}$$

that is independent of the azimuthal direction ψ of $\mathbf{Q}$ by rotation invariance. This distribution also arose naturally in the reaction operator derivation of the link cluster theorem for multiple elastic scattering in Ref. [40].

Equation (19) is clearly the intuitive factorization limit where at each order only the total accumulated momentum transfer, $\mathbf{Q}$, controls the azimuthal and momentum transfer dependence of the bremsstrahlung distribution.

By rotation invariance, $dN^{\mathrm{GB}}(\mathbf{k}, \mathbf{Q}) = dN^{\mathrm{GB}}(k, Q, \phi - \psi)$ can only depend on the k and Q azimuthal angles through their difference. After integrating over ψ, the azimuthal angle of $\mathbf{Q}$, then of course dN^{VGB} cannot depend on the azimuthal angle ϕ of $\mathbf{k}$. Therefore, it is obvious that at the single inclusive level all $v_n = 0$ vanish for $n > 0$. To observe the intrinsic fluctuating azimuthal asymmetries event by event, we turn to two-particle correlations to extract non-vanishing second moments like $\langle \cos(n(\phi_1 - \phi_2)) \rangle$. First, we discuss the bremsstrahlung contribution from recoil target participants.

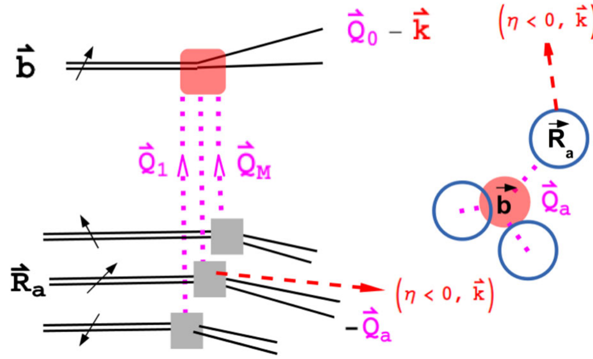

FIG. 6 (color online). (Schematic diagram corresponding to partial coherent backward $\eta < 0$ gluon bremsstrahlung from Eq. (23). At opacity order n, the azimuthal distribution is enhanced for transverse momenta $\mathbf{k}$ near the recoil momentum transfers $-\mathbf{Q}_a$, where $a = 1, \ldots, M$ labels incoherent target groups of color dipoles fragmenting into the negative rapidity region.

IV. BREMSSTRAHLUNG FROM RECOILING TARGET PARTICIPANTS

Incoherent groups of transversely overlapping recoiling target dipoles radiate gluon bremsstrahlung dominantly into the negative-rapidity $\eta < 0$ hemisphere, as illustrated in Fig. 6. In a given event when a projectile nucleon penetrates through a target nucleus A at impact parameter $\mathbf{b}$, the projectile nucleon moving with positive rapidity $Y_P > 0$ is approximated as in Ref. [37] by a color dipole with a separation $\mathbf{d}_0 = \hat{n}_0/\mu_0$. The A target nucleons moving toward negative rapidities, $Y_T < 0$, however, are distributed with transverse coordinates $\mathbf{R}_i$, according to a Glauber nuclear profile distribution $T_A(\mathbf{R}_i) = \int dz \rho_A(z, \mathbf{R}_i)$ over a large-area $\pi A^{2/3}$ fm^2 scale. Each target nucleon dipole is assumed to have a separation $\mathbf{d}_i = \hat{n}_i/\mu_i$. Projectile target dipole-dipole interactions with low transverse momentum transfer $\mathbf{q}_i < \mu_i$ are suppressed by dipole form factors approximated by $q_i^2/(q_i^2 + \mu_i^2)$. Therefore, the projectile interacts dominantly with only nearby target dipoles in the transverse plane with $(\mathbf{R}_i - \mathbf{b})^2 \lesssim \pi\alpha^2(d_0 + d_i)^2/4 \sim \sigma_{in}$. This leads to a fluctuating number n of target participants with probability $P_n = e^{-\chi}\chi^n/n!$ that follows also from the GLV opacity expansion [40,50,53].

For a given target participant number, n, the target dipoles naturally cluster near the projectile impact parameter $\mathbf{b}$ as illustrated in Figs. 5 and 6. In a specific event, there are in general $1 \le M \le n$ overlapping clusters that radiate coherently toward the negative-rapidity $\eta < 0$ hemisphere as illustrated in Fig. 6. The distribution of the number M of recoiling coherent groups depends on $n, \mathbf{k}$, and the momentum exchanges $\mathbf{q}_i$ with the projectile that build up to the total exchange to the projectile

$$\mathbf{Q}_P = \sum_{a=1}^{M} \mathbf{Q}_a = \sum_{a=1}^{M} \left(\sum_{i \in I_a} \mathbf{q}_i \right), \tag{21}$$

where I_a is a particular subset of the n indices $i \in [1, n] = \sum_a I_a$ that the emitted gluon with transverse wave number k (and generally $\eta < 0$) cannot resolve, and $\mathbf{Q}_a = \sum_{i \in I_a} \mathbf{q}_i$ is the contribution from group I_a to the total momentum transfer to the projectile.

A simple percolation model for identifying clusters of coherently recoiling target groups of dipoles is to require that all members in a cluster have separation $\mathbf{R}_{ij} = \mathbf{R}_i - \mathbf{R}_j$ in the transverse plane in a modulus that is less than the produced gluon transverse momentum resolution scale, i.e.,

$$R_{ij} \lesssim d(k) = \frac{c}{k} \tag{22}$$

where $c \sim 1$ is of order unity. If $i \in I_a$ and $j \in I_a$ as well as $j \in I_b$, then j is added to I_a if its $\langle d_{ij} \rangle_{i \in I_a} < \langle d_{ij} \rangle_{i \in I_b}$. The M clusters are percolation groups in the above sense. Of course, many other variants of transverse clustering algorithms exist. For our purpose of illustrating analytically dynamical sources v_n in $p + A$ compared to peripheral $A + A$, it suffices to study the dependence of v_n on the number of independent recoil antennas M with $\langle n \rangle = N$ fixed by Glauber participant geometry. In future applications via Monte Carlo generators such as HIJING [31], the sensitivity of results to more realistic multi-beam-jet geometric fluctuations can be studied. Note that independent target participant beam jet clusters are cylindrical cuts into the target frame near the impact parameter $\mathbf{b}$ with diameters $\sim 1/k$. We expect typically $M \sim 2$–4 independent recoil clusters even for the most central $p + A$ collisions, as illustrated in Figs. 5 and 6. This picture is similar to the CGC model picture, except that no classical longitudinal fields are assumed in our entirely perturbative QCD dynamical bremsstrahlung approach here.

In a given event, recoil bremsstrahlung contribution to the single inclusive gluon distribution from M coherently acting but transversely resolvable target antenna clusters is given by

$$dN_T^{M,N}(\eta, \mathbf{k}; \{\mathbf{q}_j\}) \equiv \sum_{a=1}^{M} dN^{\mathrm{GB}}(\mathbf{k}, -\mathbf{Q}_a) P_a(\eta), \tag{23}$$

where $P_a(\eta)$ specifies different rapidity profile functions for each cluster required to produce the characteristic BGK [34] boost-noninvariant triangular enhancement of the rapidity density, $(dN_{pA}/d\eta)/(dN_{pp}/d\eta)$, growing toward the value $\langle n \rangle = N$ near the target rapidity Y_T and dropping toward unity near the projectile rapidity Y_p.

In the special doubly coherent projectile and target limit with $M = 1$, $dN_T^{1,N}$ reduces to

$$dN_T^{1,N}(\eta, \mathbf{k}; \{\mathbf{q}_i\}_n) \equiv dN^{\mathrm{GB}}(\mathbf{k}, -\mathbf{Q}_P) P_T(\eta), \tag{24}$$

with $P_T(\eta) = \sum_a P_a(\eta)$. Note that in the high-energy small $x^- \propto \exp[Y_T - \eta]$ gluon saturation dynamics correlates $\mathbf{Q}_P$ with rapidity η instead of the simple factorization assumed in Eq. (24). In our simple perturbative dipole picture, this correlation can be implemented parametrically by taking $\mu_i(\eta) \propto Q_s(\eta, A)$ [24,42,47].

The fully coherent projectile bremsstrahlung contribution is

$$dN_P^{M,N}(\eta, \mathbf{k}; \{\mathbf{q}_i\}) \equiv dN^{\mathrm{GB}}(\mathbf{k}, +\mathbf{Q}_P) P_0(\eta). \tag{25}$$

For $p + p$ scattering with $M = N = 1$, the sum reduces in the CM to

$$dN_{pp} = dN^{\mathrm{GB}}(\mathbf{k}, +\mathbf{Q}_P) P_P(\eta) + dN^{\mathrm{GB}}(\mathbf{k}, -\mathbf{Q}_P) P_P(-\eta), \tag{26}$$

which is symmetric with respect to changing the sign of the total momentum transfer, $\mathbf{Q}_P$, as well as to reflecting η.

In the more general partially coherent target case with $1 < M \leq N$ independent clusters of dipole antennas, the total single-inclusive radiation distribution in mode $(\mathbf{k}_1, \eta_1)$ is

$$\begin{aligned} dN^{M,N} &= dN_P^N(\eta, \mathbf{k}_1; \mathbf{Q}_P) + dN_T^{M,N}(\eta, \mathbf{k}_1; \{\mathbf{Q}_a\}) \\ &= \sum_{a=0}^{M} \frac{B_{1a}}{(\mathbf{k}_1 + \mathbf{Q}_a)^2 + \mu_a^2}, \end{aligned} \tag{27}$$

where we define $\mathbf{Q}_0 \equiv -\mathbf{Q}_P = -\sum_a \mathbf{Q}_a$ to be able to include the projectile contribution in the summation over target clusters. The numerator factor B_{ia} is defined using Eqs. (5) and (6) to be

$$B_{ia} \equiv F_{k_i, Q_a} P_a(\eta_i). \tag{28}$$

For a fixed set $\mathbf{Q}_a = (Q_a, \psi_a)$ of independent recoil momenta, the single-gluon-inclusive azimuthal Fourier moments $\langle \cos(n\phi) \rangle$ are given by linear combinations of $v_n^{\mathrm{GB}}(k_1, Q_a) \cos(n\psi_a)$ from Eqs. (7)–(12). However, since all the terms in the sum contribute with one of $M + 1$ $\cos(n\psi_a)$ factors, averaging over rotations $\psi_a \to \psi_a + \theta$ again causes all ensemble-averaged $\langle v_n \rangle = 0$ to vanish for $n \geq 1$. In order to extract information about the relative *fluctuating* v_n, we therefore turn to two-gluon correlations in the next section.

V. MULTIGLUON CUMULANT AZIMUTHAL HARMONICS, $v_n\{2\ell\}$, FROM COLOR SCINTILLATION ANTENNA (CSA) ARRAYS

Multiple bremsstrahlung gluons are radiated over long ranges ("ridges") in $Y_T < \eta_i < Y_P$ from multiple kinematically and transverse-space-correlated beam jets that form "color scintillation antenna" (CSA) arrays that fluctuate from event to event. Depending on the transverse space geometry, $\mathbf{R}_a$, and the transverse momentum transfers, $\mathbf{Q}_a$, and their distributions, the CSA bremsstrahlung leads to fluctuating patterns of azimuthal correlations among the radiated gluons. Gluon bremsstrahlung from a single beam jet color dipole antenna builds up a "near side" correlations. Kinematic recoil momentum correlations between N

participant targets and the projectile antennas, however, also naturally radiate with $k^2 \sim N\mu^2$ in complex fluctuating azimuthal harmonic bremsstrahlung patterns. At very high transverse momenta $k^2 \gg M\mu^2$, collinear factorized back-to-back hard jet production dominates over multiple beam jet bremsstrahlung and leads to very strong away-side $n = 1$ correlations that must be subtracted in order to reveal the moderate $k^2 \lesssim M\mu^2$ correlations that we compute here. We also assume that we can neglect a possibly large-magnitude transverse isotropic nonperturbative bulk background through appropriate experimental mixed event subtraction schemes.

Assuming that M antenna clusters out of the $N = N_T^{\mathrm{part}}(\mathbf{b})$ target participants radiate independently—i.e., assuming that each cluster in the CSA array produces approximately a semiclassical coherent state of gluon radiation with random phase with respect to other clusters (see analogous partially coherent pion interferomentry formalism in Ref. [54]), the even-numbered 2ℓ inclusive gluon distribution factorizes as

$$dN^M_{2\ell}(\eta_1, \mathbf{k}_1, \ldots, \eta_{2\ell}, \mathbf{k}_{2\ell}) = \prod_{i=1}^{2\ell} \left(\sum_{a_i=0}^{M} \frac{B_{k_i a_i}}{A_{k_i a_i} - \cos(\phi_i + \psi_{a_i})} \right), \tag{29}$$

where B_{ia} is defined in Eq. (28) and again the summation range includes the projectile $a = 0$ contribution with $\mathbf{Q}_0 \equiv -\mathbf{Q}_P$. We emphasize that the total gluon inclusive has in addition to $dN^M_{2\ell}$ an isotropic $dN^{non.pert.}_{2\ell}$ and a highly away-side-correlated $dN^{dijet}_{2\ell}$ component that we assume can be subtracted away. Implicitly, we also assume here the greatly simplified "local parton hadron" duality hadronization prescription as in CGC models. Of course, in CGC saturation models the details, especially the x, A, and $\mathbf{b}$ will differ, but it is useful to explore here the basic consequences of this simple analytic model to get a feeling of how much of the azimuthal fluctuation phenomenology may have its roots in low-order Low-Nussinov/Gunion-Bertsch pQCD interference phenomena. Quenching of signals due especially to more realistic hadronization phenomenology [30,31,39] in the few GeV minijet scale will also need to be investigated in the future.

Even with an uncorrelated gluon-number-coherent state product ansatz for the multigluon-inclusive distribution above, the even-numbered $m = 2\ell$ gluons with $(\mathbf{k}_1, \eta_1)$ to $(\mathbf{k}_m, \eta_m)$ become correlated through the CSA geometric and kinematic recoil correlations.

Consider, for example, the $M = 2$ case (see Appendix B) of two recoiling target dipoles antennas that emit $\mathbf{k}_1$ preferentially near $-\mathbf{Q}_1 = (q_1, \psi_1 + \pi)$ and near $-\mathbf{Q}_2 = (q_2, \psi_2 + \pi)$, at two different recoil azimuthal angles $\psi_1 + \pi$ and $\psi_2 + \pi$, while the projectile dipole emits $\mathbf{k}_2$ preferentially near $\mathbf{Q}_P = \mathbf{Q}_1 + \mathbf{Q}_2$ at a third ϕ_P azimuthal angle. Such a three-color antenna system then naturally leads to two-particle triangularity $v_3\{2\} \equiv \langle\cos(3(\phi_1 - \phi_2))\rangle \neq 0$ due to dynamical correlations between $\mathbf{k}_1$ and $\mathbf{k}_2$. As we also show below in Sec. V, special cases of Z_n symmetric antenna arrays illustrate "perfect pitch" bremsstrahlung with $v_{n'}\{2\} = \delta_{nn'} v_n^{Z_n}\{2\}$ two-particle harmonic.

Consider in detail the prototype $M = 1$ VGB antenna case again, but for 2ℓ gluon cumulant nth relative harmonic moments for a fixed Q impulse from

$$\begin{aligned}
f_n^{M=1}\{2\ell\} &\equiv \langle e^{+in\{\sum_{i=1}^{\ell} \phi_i\}} e^{-in\{\sum_{j=\ell+1}^{2\ell} \phi_j\}} \rangle f_0^{M=1}\{2\ell\} \\
&= \prod_{i=1}^{\ell} \left(\int \frac{d\phi_i}{2\pi} \frac{B_{k_i Q} e^{+in\phi_i}}{A_{k_i Q} - \cos(\phi_i + \psi_Q)} \right) \prod_{j=\ell+1}^{2\ell} \left(\int \frac{d\phi_j}{2\pi} \frac{B_{k_j Q} e^{-in\phi_j}}{A_{k_j Q} - \cos(\phi_j + \psi_Q)} \right) \\
&= \prod_{i=1}^{\ell} (e^{in\psi_Q} (z_{k_i Q})^n f_{0,k_i,Q}) \prod_{j=\ell+1}^{2\ell} (e^{-in\psi_Q} (z_{k_j Q})^n f_{0,k_j,Q}) \\
&= f_0^{M=1}\{2\ell\} \prod_{i=1}^{2\ell} (v_1^{\mathrm{GB}}(k_i, Q))^n.
\end{aligned} \tag{30}$$

Note that by construction, $f_n^M\{2\ell\}$ are $SO(2)$ rotation invariant about the beam axis, and thus independent, unlike odd moments of the random orientation, ψ_Q, of the reaction plane defined by the transverse momentum transfer $\mathbf{Q}$. Here $z_{k_i Q} = A_{k_i Q} - \sqrt{A^2_{k_i Q} - 1}$ are the poles inside the unit circle that contribute to the nth harmonics. For an odd number of gluons, all harmonics vanish, but for even numbers all harmonics, both even and odd, are generated already by one $M = 1$ color GB bremsstrahlung antenna. For $M = 2$, two recoiling GB antennas $\mathbf{Q}$ and $-\mathbf{Q}$, all odd

$n = 1, 3, \ldots$ moments vanish by symmetry. An odd number of antennas M is needed to generate odd n harmonics through an even number of gluon correlators.

In the "mean recoil" approximation $Q \approx \bar{Q}$, we see that a single GB antenna satisfies the generalized power scaling law in case subsets of the 2ℓ gluons have identical momenta. Suppose there are $1 \leq L \leq 2\ell$ distinct momenta K_r with $r = 1, \ldots, L$ such that m_r of the 2ℓ gluons have momenta equal to a particular value K_r, such that $\sum_{r=1}^{L} m_r = 2\ell$. In this case,

$$v_n^{M=1}\{2\ell\}(k_1, \ldots, k_{2\ell}; \bar{Q}) \approx \prod_{r=1}^{L} (v_n^{\mathrm{GB}}(K_r, \bar{Q}))^{m_r} = \prod_{r=1}^{L} (v_1^{\mathrm{GB}}(K_r, \bar{Q}))^{n m_r}. \tag{31}$$

The approximate factorization and power scaling of azimuthal harmonics from CSA coherent state non-Abelian bremsstrahlung is similar to "perfect fluid hydrodynamic collective flow" factorization and scaling, but in this case no assumption about local equilibration or minimal viscosity is necessary.

Higher-order *cumulant* harmonic correlations were proposed [55–58] to help remove "nonflow" sources of correlations such as momentum conservation, back-to-back dijet, and Bose statistics effects and to isolate true collective bulk fluid flow azimuthal asymmetries. The 2ℓ-particle cumulant suppresses the "nonflow" contribution by eliminating the correlations which act between fewer than 2ℓ particles (see, e.g., Fig. 9 of Ref. [57]). The first few cumulants for $2\ell = 2, 4, 6$ (notation from Refs. [56,57]) are

$$\begin{aligned}
(v_n\{2\})^2 &\equiv \langle e^{in(\phi_1-\phi_2)}\rangle \equiv \langle |v_2|^2\rangle, \\
(v_n\{4\})^4 &\equiv \langle -e^{in(\phi_1+\phi_2-\phi_3-\phi_4)}\rangle + 2\langle e^{in(\phi_1-\phi_3)}\rangle\langle e^{in(\phi_2-\phi_4)}\rangle = 2\langle |v_2|^2\rangle^2 - \langle |v_n|^4\rangle, \\
(v_n\{6\})^6 &\equiv (\langle e^{in(\phi_1+\phi_2+\phi_3-\phi_4-\phi_5-\phi_6)}\rangle - 9\langle |v_2|^2\rangle\langle |v_n|^4\rangle + 12\langle |v_2|^2\rangle^3)/4.
\end{aligned} \tag{32}$$

The observed [57] near equality of $v_n\{2\ell\}$ for $\ell = 2, 3, 4$ in Pb + Pb at LHC has been interpreted as evidence supporting perfect fluid flow. The similarity of "elliptic flow" $v_2\{4\}(p_T)$ in p + Pb and Pb + Pb observed by ATLAS [4] and also for "triangular flow" $v_3\{4\}(p_T)$ by CMS [2] has been interpreted as further evidence for perfect fluidity even on subnucleon scales in p + Pb.

However, we see that color bremsstrahlung exhibits similar scaling of azimuthal harmonic cumulants in the mean recoil approximation. In the case that all 2ℓ gluon momenta are identical,

$$\bar{v}_n\{2\ell\} \equiv (v_m^{M=1}\{2\ell\}(k, \ldots, k; \bar{Q}))^{n/m}, \tag{33}$$

which implies in the above notation that

$$\langle |v_n|^4\rangle = \langle |v_2|^2\rangle^2, \tag{34}$$

$$\langle |v_6|^6\rangle = \langle |v_2|^2\rangle\langle |v_n|^4\rangle = \langle |v_2|^2\rangle^3, \tag{35}$$

and similarly for all cumulants. Therefore, color bremsstrahlung obeys the *similar* azimuthal harmonic cumulant independence on the number of gluons 2ℓ used to determine the harmonic moments, as does the perfect hydrodynamic flow hypothesis. However, in our CSA bremsstrahlung case, the apparent "flow" effect comes purely from zero-temperature coherent state (semiclassical) non-Abelian wave interference effects that depend on the transverse geometric arrangement of CSA arrays.

For the $p + A$ case of multiple $M > 1$ independent target cluster CSA arrays, the cumulant harmonic moments depend in a more complex way on the particular geometric and recoil correlations defining the CSA. Special analytic CSA cases for $v_2\{2\}$ corresponding to idealized Z_n and Gaussian CSA arrays are discussed in the following two sections.

VI. SPECIAL CASE OF Z_n CSA BREMSSTRAHLUNG

As seen in Appendix B from Eq. (B4), it is clear that particularly simple special cases of color antenna arrays, where $M = n - 1$ target beam jet clusters all have similar numbers of recoiling target partons $m_a = N/M = N/(n-1)$, transfer all $n = M + 1$ projectiles, and the target beam jets recoil with similar momentum transfers, $Q_a^2 = N/M\mu^2$, but with specially spaced azimuthal angles, $\{\psi_a\} = 2\pi a/n$.

These particular color antenna arrays, that we will refer to as Z_n color scintillation arrays (CSA), have a special discrete azimuthal rotation symmetry corresponding to the finite group of n roots of unity;

$$Z_n = \left\{ z_{a,n} = e^{i2\pi a/n} | a = 0, \ldots, n-1; \sum_{a=0}^{n-1} z_{a,n} = 0 \right\}. \tag{36}$$

For these Z_n CSA geometries of projectile and target color dipole antennas, the double sum over a and b is trivial because

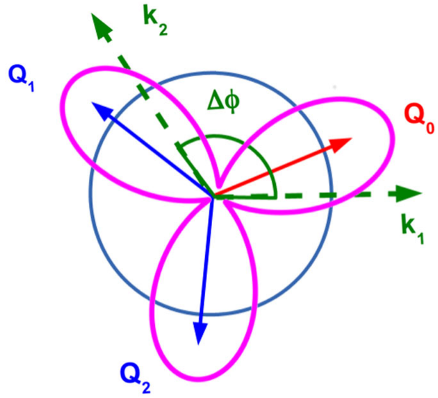

(a)

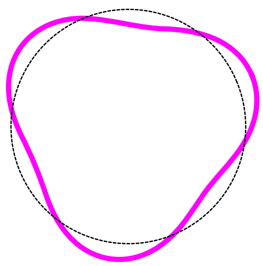

(b)

FIG. 7 (color online). Example illustrating apparent perfect "triangular flow" but arising entirely from non-Abelian bremsstrahlung sourced by color scintillation antenna (CSA) arrays. In this case, $M = 2$ target beam jet clusters recoil off a projectile beam jet with $\mathbf{Q}_0 = -\sum_{a=1}^{M} \mathbf{Q}_a$, and all Q_a are assumed to have same magnitude but spaced in azimuth by $2\pi/3$. A Z_3 CSA radiates only $n = 3$ harmonics: $v_n\{2\}(k_1, k_2) = \delta_{n,3} v_3^{\mathrm{GB}}(k_1, Q_0) v_3^{\mathrm{GB}}(k_2, Q_0)$. Part (a) shows an extreme case with $v_3 = 0.45$, while (b) shows a more realistic $v_3 = 0.07$ case. An arbitrary isotropic soft nonperturbative background is assumed to be subtracted out.

$$\cos(n(\psi_a - \psi_b)) = \cos(2\pi(a - b)) = 1, \tag{37}$$

and thus all $(M + 1)^2 = n^2$ terms are identical. Note that Eq. (37) is invariant to global $SO(2)$ simultaneous rotations of all antennas.

What is remarkable about Z_{M+1} symmetric CSAs is that due to the orthogonality properties of the z_{an} phases,

$$\sum_{a=1}^{n-1} z_{a,n}^k = n\delta_{k,n}, \tag{38}$$

$$\sum_{a=1}^{n-1} (z_{a,n})^k (z_{a,n}^*)^{k'} = n\delta_{k,k'}, \tag{39}$$

all harmonics except $n = M + 1$ vanish. The Z_n CSAs thus scintillate with "perfect" n-harmonic azimuthal correlations. For Z_n CSAs, the two-particle relative Fourier moments $v_n\{2\}$ simply factor into a product of single-particle moments $v_n^{\mathrm{GB}}(k_i, Q_0, 0)$, because the n complex

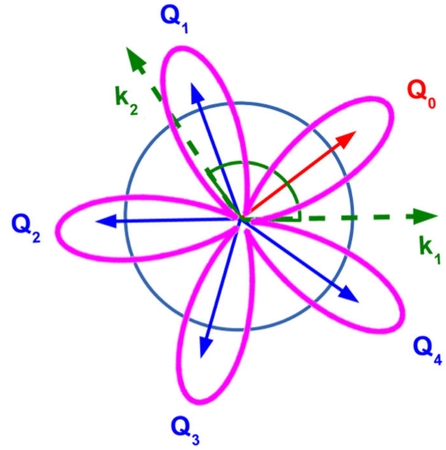

(a)

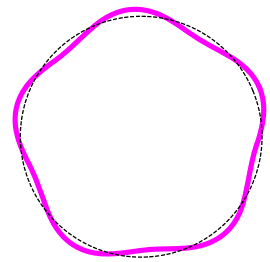

(b)

FIG. 8 (color online). As in Fig. 7, but for a Z_5 symmetric CSA that radiates an apparent "perfect pentatonic flow" pattern with $v_n\{2\}(k_1, k_2) = \delta_{n,5} v_5^{\mathrm{GB}}(k_1, Q_0) v_5^{\mathrm{GB}}(k_2, Q_0)$. Part (a) shows an extreme $v_5 = 0.45$ case, while part (b) shows a more realistic $v_5 = 0.03$ case.

$Q_a = Q_0 z_{a,n}$ form a regular polygon with equal radii, as illustrated for an $n = 5$ "star fish" antenna array in Fig. 7, that generates a perfect $\cos(5(\phi_1 - \phi_2))$ two-particle azimuthal correlation.

For roots of unity CSA color antenna geometries, all $M + 1$ antennas receive the same $Q_a^2 = Q_0^2 = N/(n-1)\mu^2$ momentum transfer and produce the same single-particle $v_{M+1}^{\mathrm{GB}}(k, Q_0, 0)$ harmonics. Since the two-particle harmonics vanish except for $n = M + 1$,

$$\begin{aligned} &v_n^{M,N}\{2\}(k_1, k_2) \xrightarrow{Z_n} \delta_{n,M+1} v_{M+1}^{\mathrm{GB}}(k_1, Q_0) v_{M+1}^{\mathrm{GB}}(k_2, Q_0), \\ &\frac{v_n^{M,N}\{2\}(k_1, k_2)}{v_{M+1}^{\mathrm{GB}}(k_2, Q_0)} \xrightarrow{Z_n} \delta_{n,M+1} (v_1^{\mathrm{GB}}(k_1, Q_0))^{M+1}, \end{aligned} \tag{40}$$

and for $n = M + 1$, $v_{M+1}^{M,N}\{2\}(k_1, k_2)$ is reduced to simply the product of single-GB CSA moments at k_1 and k_2.

Examples of Z_n radiation patterns for $n = 3, 5$ for extremely high $v_n = 0.45$ in parts (a) and more realistic $v_3 = 0.7$ and $v_5 = 0.03$ from Fig. 1 are shown in Figs. 7 and 8.

VII. SPECIAL CASE OF GAUSSIAN CSA BREMSSTRAHLUNG

Another simple limit is found when the recoil azimuthal angles ψ_a are in random $[0, 2\pi]$ and the $\mathbf{Q}_a$'s are distributed with a Gaussian of the same width squared $\langle Q_a^2\rangle = Q_T^2 = (N/M)\mu^2$ for $a \in [1, \ldots, M]$. In this antenna array, the projectile $\mathbf{Q}_0$ is also Gaussian distributed with zero mean, but with an enhanced second moment,

$$\langle Q_0^2\rangle = MQ_T^2 = N\mu^2. \tag{41}$$

Unlike for perfect nth-harmonic antenna arrays with Eq. (37), in the random Gaussian distributed case

$$\cos(n(\psi_a - \psi_b)) = \delta_{a,b}, \tag{42}$$

and so only the $a = b$ diagonal terms contribute. All $a \geq 1$ target terms are identical, and only the projectile contribution is enhanced due to $\langle Q_0^2\rangle/Q_T^2 = M$ random walk exchanges from each cluster. In this case, Eq. (B4) reduces to

$$\begin{aligned} f_n^{N,M}(k_1, k_2) \overset{\text{Gauss}}{\to} \int d^2\mathbf{Q}\left\{\frac{\exp[-\mathbf{Q}^2/(2N\mu^2)]}{2\pi N\mu^2} + M\frac{\exp[-\mathbf{Q}^2/(2(N/M)\mu^2)]}{2\pi(N/M)\mu^2}\right\}\{B_{1Q}B_{2Q}f_{0,1,Q}f_{0,2,Q} \\ \times v_n^{\text{GB}}(k_1, Q)v_n^{\text{GB}}(k_2, Q)\}, \end{aligned} \tag{43}$$

$$f_n^{N,M}(k, k) \overset{\text{Gauss}}{\to} \int d^2\mathbf{Q}\left\{\frac{\exp[-Q^2/(2N\mu^2)]}{2\pi N\mu^2} + M\frac{\exp[-Q^2/(2(N/M)\mu^2)]}{2\pi(N/M)\mu^2}\right\}\{B_{kQ}f_{0,k,Q}v_n^{\text{GB}}(k, Q)\}^2. \tag{44}$$

We have suppressed target and projectile kinematic rapidity factors.

To get a feeling for the magnitude of the two particle azimuthal moments, we can approximate Q in the integrand outside the Gaussian weights by its rms $\Delta Q = \sqrt{\langle Q^2\rangle}$ and perform the normalized integral over the Gaussians to estimate

$$\begin{aligned} \sqrt{f_n^{N,M}(k, k)} \approx \left(\frac{C_R\alpha_s\mu^2}{\pi^2 k^2}\right)\left\{\frac{1}{(N+1)\mu^2}\frac{(v_1^{\text{GB}}(k, \sqrt{N}\mu))^n}{((k^2 + (N+1)\mu^2)^2 - 4Nk^2\mu^2)^{1/2}}\right. \\ \left. + \frac{M}{(N/M+1)\mu^2}\frac{(v_1^{\text{GB}}(k, \sqrt{N/M}\mu))^n}{((k^2 + (N/M+1)\mu^2)^2 - 4(N/M)k^2\mu^2)^{1/2}}\right\}. \end{aligned} \tag{45}$$

The rapidity dependence corresponding to the BGK [34] triangular rapidity enhancement $N(Y_P - \eta)/(Y_P - Y_T)$ of the single inclusive multiplicity toward the target fragmentation region is suppressed above to simplify the result. In addition, we emphasize that the mostly nonperturbative low-k background is ignored in our simplified consideration here. Full account for that background will require implementation of the above nonisotropic soft bremsstrahlung in an event generator such as HIJING.

A qualitative BGK [34] rapidity dependence for the target cluster number $M(\eta)$ that ignores the c/k resolution scale considerations discussed in Eq. (22) can be estimated by identifying $N = \chi = \int dz\rho_A(z, \mathbf{b})$ with the opacity as a function of b and taking

$$M_{\text{BGK}}(\eta) \sim \chi(Y_P - \eta)/(Y_P - Y_T)(1 - e^{Y_T - \eta})^{n_f}. \tag{46}$$

The main feature expected from such a BGK [34] rapidity dependence of the target cluster number is that the mean transverse momentum radiated gluons from combined projectile and target bremsstrahlung gluons grows toward the projectile rapidity region dominated by the projectile contribution. This predicts then that the peak k_* of the $v_n(k)$ moments moves to larger

$$k_*^2 \approx \frac{N + M(\eta)}{1 + M(\eta)}\mu^2 \tag{47}$$

as η is increased.

VIII. HIJNG MONTE CARLO COLOR SCINTILLATING BEAM JET ARRAYS

To get a realistic estimate for the magnitudes and systematics of pQCD VGB induced harmonics in realistic $p+p, p+A, A+A$ collisions, we have to embed the anisotropic recoil bremsstrahlung gluons into phenomenological Lund strings with a hadronization scheme that has been tuned to reproduce low-p_T *ϕ-averaged* inclusive hadronic observables in $e^+ + e^-$, $e + p$, $p + p$, $p + A$, as well as $A + A$. The HIJING Monte Carlo event generator is one such model based on the LUND [30] string model and the PYTHIA and JETSET [39] Monte Carlo models.

Simple local parton-hadron duality prescription as used in CGC cannot be expected to predict quantitative hadron-mass-dependent moderate $p_T < 2$ GeV anisotropy moments over three decades of $\sqrt{s}$. The advantage of Monte Carlo event generators built on multidecade phenomenological analysis is that they summarize the world data by taking into account the particle data book, quantum number, and energy momentum conservation and numerous Standard Model dynamical details. Of course, they do not purport to cover all possible phenomena.

A key feature missing in HIJING and most other event generators for $A + B$ collisions so far are basic pQCD azimuthal anisotropies at the moderate $p_T < 2$ GeV scale that are so clearly predicted by GB and generalized VGB bremsstrahlung models. What is included in most event generators are strong back-to-back jet azimuthal anisotropies due to collinear factorized pQCD mini- and hard jet production above some saturation scale $p_T > p_0 \sim 2$ GeV. As currently implemented, HIJING takes into account softer-scale $k < p_0$ gluons phenomenologically via random transverse LUND string "wiggles" using ARIADNE [38], but HIJING neglects the basic pQCD azimuthal recoil correlations predicted by VGB color bremsstrahlung. An current open question is the magnitude of radiated anisotropies that would arise when the ARIADNE part of the JETSET code is replaced by VGB anisotropic bremsstrahlung derived in this paper. We intend to address this numerically intensive problem elsewhere.

IX. CONCLUSIONS

In summary, we applied the GLV reaction operator approach to Vitev-Gunion-Bertsch (VGB) boundary conditions in order to compute to all orders in nuclear opacity the non-Abelian gluon bremsstrahlung for event-by-event fluctuating semisoft beam jets produced in high-energy nuclear collisions. We derived analytic expressions for the azimuthal Fourier cumulant moments $v_n\{2\ell\}$ as a function of the gluon transverse momenta and rapidities, $\{\mathbf{k}_i, \eta_i\}$, in terms of remarkably simple single-gluon beam jet GB bremsstrahlung harmonics. These moments were shown to obey power-law scaling laws similar to those observed recently in high-energy $p + A$ reactions at RHIC and at LHC as a function of the target participant clusters geometry. Multiple clusters of projectile and target beam jets form color scintillation antenna (CSA) arrays that radiate gluons with characteristic boost-noninvariant trapezoidal rapidity distributions in asymmetric $B + A$ nuclear collisions. The intrinsically azimuthally anisotropic and long-range in η nature of the non-Abelian bremsstrahlung leads to v_n moment systematics that are remarkably similar to those predicted by perfect fluid hydrodynamic models. However, in our case, they arise entirely from non-Abelian wave interference phenomena sourced by the fluctuating CSA of multiple beam jets.

We presented examples of simple solvable CSA models and showed that our analytic nonflow bremsstrahlung solutions for $v_n\{2\ell\}$ are similar to recent numerical saturation model predictions but differ by predicting a simple power-law hierarchy of both even and odd $v_n\{2\ell\}$ without invoking essential details of k_T factorization. However, CGC saturation evolution is expected to be important for future quantitative comparisons to data. The basic CSA mechanism can be tested via its predicted systematics involving boost-noninvariant trapezoidal BGK η rapidity-dependent substructures involved in $B + A$ reactions.

Non-Abelian beam jet CSA bremsstrahlung, investigated in this paper, may provide a partial analytic solution to the beam energy scan (BES) puzzle of the observed near $\sqrt{s}$ independence of the azimuthal moments down to a very low CM energy of $\sim$10 AGeV, where large-x valence-quark beam-jet physics dominates over gluon production in inelastic dynamics. Recoil bremsstrahlung from multiple independent CSA clusters also provides a natural qualitative pQCD explanation for the surprising similarity of v_n in $p(D) + A$ and noncentral $A + A$ at same $dN/d\eta$ multiplicity observed at RHIC and LHC.

This pQCD-based model shows that the uniqueness of the perfect fluid interpretation of $p + A$ and $B + A$ azimuthal correlation data cannot be taken for granted. However, a great deal of work remains to sort out quantitatively the fraction of the observed $v_n\{2\ell\}$ azimuthal harmonic systematics that can be ascribed to final-state hydrodynamic collective flow versus initial-state QCD coherent state color scintillating interference wave phenomena.

ACKNOWLEDGMENTS

M. G. is grateful to W. Busza, J. Harris, J. Jia, A. Poszkanzer, H. J. Ritter, and N. Xu for discussion related to RHIC and LHC flow experiments, and to A. Dumitru, T. Lappi, L. McLerran, J. Noronha, H. Stoecker, G. Torieri, and R. Venugopalan for critical discussions related to hydrodynamic and QCD field theory models of $A + A$ correlations. M. G. acknowledges support from U.S. Department of Energy Nuclear Science Grant No. DE-FG02-93ER40764, partial sabbatical support from LBNL under DOE Grant No. DE-AC02-05CH11231, the Yukawa Institute for Theoretical Physics, Kyoto University, support from the YITP-T-13-05 on "New Frontiers in QCD" workshop, and sabbatical support from the MTA Wigner RCP, Budapest, where this work was finalized. P. L. and T. B. acknowledge support from Hungarian OTKA Grants No. K81161, No. K104260, No. NK106119, and No. NIH TET_12_CN-1-2012-0016. I. V. was supported in part by the U.S. Department of Energy, Office of Science, Office of Nuclear Physics.

APPENDIX A: THE LINKED CLUSTER THEOREM FOR COHERENT VGB GLUON BREMSSTRAHLUNG

To derive the link cluster theorem for the coherent limit of VGB, we introduce the shorthand notation for the integrations over momentum transfers:

$$\prod_{j=1}^{n}\int d(w_j-\delta_j)\equiv\int\prod_{j=1}^{n}d^2\mathbf{q}_j\left(\frac{1}{\sigma_{el}}\frac{d\sigma_{el}}{d^2\mathbf{q}_j}-\delta^2(\mathbf{q}_j)\right), \tag{A1}$$

which have the convenient properties $\int dw_j=\int d\delta_j=1$ and $\int d(w_j-\delta_j)=0$. This makes it possible to discard any terms in the integrand that do not depend simultaneously on all n $\mathbf{q}_j$ momenta at fixed opacity order n. Using this shorthand and $\mathbf{C}_{jn}$ notation from Eq. (16), we rewrite the right-hand side of Eq. (18) as

$$\begin{aligned}\mathrm{VGB}&=\frac{C_R\alpha_s}{\pi^2}\sum_{n=1}^{\infty}\frac{\chi^n}{n!}\left[\prod_{j=1}^{n}\int d(w_j-\delta_j)\right]\\&\quad\times(\mathbf{C}_{2n}-\mathbf{C}_{1n})\cdot[(\mathbf{C}_{2n}-\mathbf{C}_{1n})+2(\mathbf{C}_{3n}-\mathbf{C}_{2n})+\cdots+2(\mathbf{C}_{(n+1)n}-\mathbf{C}_{nn})]\\&=\frac{C_R\alpha_s}{\pi^2}\sum_{n=1}^{\infty}\frac{\chi^n}{n!}\left[\prod_{j=1}^{n}\int d(w_j-\delta_j)\right](\mathbf{C}_{2n}-\mathbf{C}_{1n})\cdot[(\mathbf{C}_{2n}-\mathbf{C}_{1n})+2(\mathbf{H}-\mathbf{C}_{2n})]\\&=\frac{C_R\alpha_s}{\pi^2}\sum_{n=1}^{\infty}\frac{\chi^n}{n!}\left[\prod_{j=1}^{n}\int d(w_j-\delta_j)\right][-(\mathbf{H}-\mathbf{C}_{2n})+(\mathbf{H}-\mathbf{C}_{1n})]\cdot[(\mathbf{H}-\mathbf{C}_{2n})+(\mathbf{H}-\mathbf{C}_{1n})]\\&=\frac{C_R\alpha_s}{\pi^2}\sum_{n=1}^{\infty}\frac{\chi^n}{n!}\left[\prod_{j=1}^{n}\int d(w_j-\delta_j)\right]\{|\mathbf{H}-\mathbf{C}_{1n}|^2-|\mathbf{H}-\mathbf{C}_{2n}|^2\}\\&=\frac{C_R\alpha_s}{\pi^2}\sum_{n=1}^{\infty}\frac{\chi^n}{n!}\left[\prod_{j=1}^{n}\int d(w_j-\delta_j)\right]|\mathbf{H}-\mathbf{C}_{1n}|^2\\&=\sum_{n=1}^{\infty}\frac{\chi^n}{n!}\left[\prod_{j=1}^{n}\int d(w_j-\delta_j)\right]\left(\int d^2\mathbf{Q}\delta^2(\mathbf{Q}-(\mathbf{q}_1+\cdots+\mathbf{q}_n))\right)\left\{\frac{C_R\alpha_s}{\pi^2}\frac{\mathbf{Q}^2}{k^2(\mathbf{k}-\mathbf{Q})^2}\right\}.\end{aligned} \tag{A2}$$

Here, we use the notation $\mathbf{H}\equiv\mathbf{C}_{(n+1),n}\equiv\mathbf{k}/k^2$ to denote the "hard" vacuum radiation amplitude that shows up at zeroth order in opacity in the case of final-state induced radiation in GLV [50]. Note that in this notation convention $\mathbf{B}^n_{(n+1),n)}\equiv\mathbf{H}-\mathbf{C}_{nn}$.

Note that $\int d(w_j-\delta_j)=0$, and therefore for $j=1$ the integral of $-|\mathbf{H}-\mathbf{C}_{2n}|^2$ automatically vanishes. Note further that the $|\mathbf{H}-\mathbf{C}_{1n}|^2$ integrand depends only on $\mathbf{k}$ and the *total* accumulated $\mathbf{Q}=\sum_{i=1}^{n}\mathbf{q}_i$ momentum transfer. Thus, the integrand is symmetric under arbitrary permutations of the indices. This is the key to obtaining the linked cluster rearrangement, because out of the 2^n combinations of the w_j and minus delta functions $-\delta_i$, all combinations with the same number m of $\int dw$ and $n-m$ of $\int d\delta$ integrations give the same contribution. At fixed opacity order n, the 2^n combinations of integrals reduce to sum over only n integrals of the form $n!/(m!(n-m)!)\int dw_1\ldots dw_m(-1)^{n-m}|B^m_{1m}|^2$. Therefore,

$$\frac{dN^{\mathrm{VGB}}_{\mathrm{coh}}}{d\eta d^2\mathbf{k}}=\sum_{n=1}^{\infty}\frac{\chi^n}{n!}\sum_{m=1}^{n}\frac{(-1)^{n-m}n!}{m!(n-m)!}\int d^2\mathbf{Q}\left[\int dw_1\ldots dw_m\delta^2(\mathbf{Q}-(\mathbf{q}_1+\cdots+\mathbf{q}_m))\right]\left\{\frac{C_R\alpha_s}{\pi^2}\frac{Q^2}{k^2(\mathbf{k}-\mathbf{Q})^2}\right\}. \tag{A3}$$

Changing summation variables from $\infty>n\geq1$ and $n\leq m\geq1$ to $\infty>\ell=n-m\geq0$ and $\infty>m\geq1$, the double sum $\sum_{\ell=0}^{\infty}\sum_{m=1}^{\infty}$ factorizes, and the sum over ℓ produces a factor $\exp[-\chi]$ corresponding to the probability of no scattering. Therefore, Eq. (A3) leads to the link cluster theorem in Eq. (19) for the multiple-collision VGB generalization of Gunion-Bertsch gluon bremsstrahlung.

APPENDIX B: TWO-GLUON BREMSSTRAHLUNG AZIMUTHAL HARMONICS $v_n\{2\}$

For the two-gluon case, azimuthal harmonic correlations can be directly derived in another way by integrating over both $\phi_1=\Phi+\Delta\phi/2$ and $\phi_2=\Phi-\Delta\phi/2$, keeping the relative azimuthal angle $\Delta\phi=\phi_1-\phi_2$ fixed and weighing the integrand by $\cos(n\Delta\phi)$ from

$$f_n^M\{2\}(k_1,k_2) \equiv \int_{-\pi}^{\pi}\frac{d\Phi}{2\pi}\int_{-\pi}^{\pi}\frac{d\Delta\phi}{2\pi}\cos(n\Delta\phi)dN_2^M(k_1,\Phi+\Delta\phi/2,k_2,\Phi-\Delta\phi/2)$$

$$= \sum_{a,b=0}^{M} B_{1a}B_{2b}\int_{-\pi}^{\pi}\frac{d\Delta\phi}{2\pi}\cos(n\Delta\phi)\int_{-\pi}^{\pi}\frac{d\Phi}{2\pi}\frac{1}{A_{1a}-\cos(\Phi+\psi_a+\Delta\phi/2)}\frac{1}{A_{2b}-\cos(\Phi+\psi_b-\Delta\phi/2)} \tag{B1}$$

$$= \sum_{a,b=0}^{M} B_{1a}B_{2b}\int_{-\pi}^{\pi}\frac{d\Phi'}{2\pi}\frac{1}{A_{1a}-\cos(\Phi')}\int_{-\pi}^{\pi}\frac{d\Delta\phi}{2\pi}\frac{\cos(n\Delta\phi)}{A_{2b}-\cos((\Phi'+\psi_b-\psi_a)-\Delta\phi)} \tag{B2}$$

$$= \sum_{a,b=0}^{M} B_{1a}B_{2b}f_{n,2,b}\int_{-\pi}^{\pi}\frac{d\Phi'}{2\pi}\frac{\cos(n(\Phi'+\psi_b-\psi_a))}{A_{1a}-\cos(\Phi')} = \sum_{a,b=0}^{M} B_{1a}B_{2b}f_{n,2,b}f_{n,1,a}\cos(n(\psi_b-\psi_a)) \tag{B3}$$

$$= \sum_{a,b=0}^{M} B_{1a}B_{2b}f_{0,1,a}f_{0,2,b}(v_1^{\mathrm{GB}}(k_1,Q_a)v_1^{\mathrm{GB}}(k_2,Q_b))^n\cos(n(\psi_b-\psi_a)), \tag{B4}$$

where we define $\Phi' = \Phi+\psi_a+\Delta\phi/2$ and use the periodicity of the integrand to shift the Φ' range back to $[-\pi,\pi]$ in Eq. (B2), then perform the $\Delta\phi$ integral with the help of Eq. (7). We use here the shorthand notation

$$f_{n,1,a} = \int_{-\pi}^{\pi}\frac{d\Phi}{2\pi}\frac{\cos(n\Phi)}{A_{1a}-\cos(\Phi)} = (v_1^{\mathrm{GB}}(k_1,Q_a))^n f_{0,1,a}, \tag{B5}$$

$$f_{n,1,a} = \frac{(A_{k_1,Q_a}-\sqrt{A_{k_1,Q_a}^2-1})^n}{\sqrt{A_{k_1,Q_a}^2-1})}, \tag{B6}$$

$$\lim_{\mu\to 0} f_{n,1,a} = \left(\frac{k_1}{Q_a}\right)^n\frac{\theta(Q_a-k_1)}{Q_a^2-k_1^2}Q_a^2. \tag{B7}$$

[1] A. Adare *et al.* (PHENIX Collaboration), Phys. Rev. Lett. **111**, 212301 (2013).

[2] S. Chatrchyan *et al.* (CMS Collaboration), Phys. Lett. B **718**, 795 (2013).

[3] B. Abelev *et al.* (ALICE Collaboration), Phys. Lett. B **719**, 29 (2013).

[4] G. Aad *et al.* (ATLAS Collaboration), Phys. Rev. Lett. **110**, 182302 (2013); Phys. Lett. B **725**, 60 (2013).

[5] J. Adams *et al.* (STAR Collaboration), Nucl. Phys. **A757**, 102 (2005).

[6] K. Adcox *et al.* (PHENIX Collaboration), Nucl. Phys. **A757**, 184 (2005).

[7] A. Adare *et al.* (PHENIX Collaboration), Phys. Rev. Lett. **105**, 062301 (2010).

[8] K. Aamodt *et al.* (ALICE Collaboration), Phys. Lett. B **708**, 249 (2012).

[9] K. Aamodt *et al.* (ALICE Collaboration), Phys. Rev. Lett. **105**, 252302 (2010).

[10] K. Aamodt *et al.* (ALICE Collaboration), Phys. Rev. Lett. **107**, 032301 (2011).

[11] S. Chatrchyan *et al.* (CMS Collaboration), Eur. Phys. J. C **72**, 2012 (2012).

[12] G. Aad *et al.* (ATLAS Collaboration), Phys. Rev. C **86**, 014907 (2012).

[13] ATLAS Collaboration, Report No. ATLAS-CONF-2014-021, 2014, http://cds.cern.ch/record/1702976.

[14] J. Jia (private communication).

[15] L. Adamczyk *et al.* (STAR Collaboration), Phys. Rev. C **88**, 014902 (2013).

[16] P. Romatschke and U. Romatschke, Phys. Rev. Lett. **99**, 172301 (2007).

[17] M. Luzum and P. Romatschke, Phys. Rev. C **78**, 034915 (2008); Phys. Rev. Lett. **103**, 262302 (2009).

[18] B. H. Alver, C. Gombeaud, M. Luzum, and J.-Y. Ollitrault, Phys. Rev. C **82**, 034913 (2010).

[19] C. Gale, S. Jeon, B. Schenke, P. Tribedy, and R. Venugopalan, Phys. Rev. Lett. **110**, 012302 (2013).

[20] U. Heinz and R. Snellings, Annu. Rev. Nucl. Part. Sci. **63**, 123 (2013).

[21] P. Danielewicz and M. Gyulassy, Phys. Rev. D **31**, 53 (1985); T. Hirano and M. Gyulassy, Nucl. Phys. **A769**, 71 (2006).

[22] P. Bozek, Phys. Rev. C **85**, 014911 (2012); P. Bozek and W. Broniowski, Phys. Rev. C **88**, 014903 (2013); Acta Phys. Pol. B **45**, 1337 (2014).
[23] G. Basar and D. Teaney, arXiv:1312.6770.
[24] K. Dusling and R. Venugopalan, Phys. Rev. D **87**, 094034 (2013).
[25] D. Teaney, J. Lauret, and E. V. Shuryak, Phys. Rev. Lett. **86**, 4783 (2001).
[26] G. Agakichiev *et al.* (CERES/NA45 Collaboration), Phys. Rev. Lett. **92**, 032301 (2004); D. Adamova *et al.* (CERES Collaboration), Nucl. Phys. **A894**, 41 (2012).
[27] J. Auvinen and H. Petersen, Phys. Rev. C **88**, 064908 (2013); J. Phys. Conf. Ser. **503**, 012025 (2014).
[28] Y. B. Ivanov, arXiv:1401.2265.
[29] K. Dusling and R. Venugopalan, Phys. Rev. D **87**, 051502 (2013).
[30] B. Andersson, G. Gustafson, and B. Nilsson-Almqvist, Nucl. Phys. **B281**, 289 (1987).
[31] X.-N. Wang and M. Gyulassy, Phys. Rev. D **44**, 3501 (1991); M. Gyulassy and X. N. Wang, Comput. Phys. Commun. **83**, 307 (1994).
[32] R. Debbe (ATLAS Collaboration), Report No. ATLAS-CONF-2014-021, 2014.
[33] M. Gyulassy and L. McLerran, Nucl. Phys. **A750**, 30 (2005).
[34] S. J. Brodsky, J. F. Gunion, and J. H. Kuhn, Phys. Rev. Lett. **39**, 1120 (1977).
[35] A. Adil and M. Gyulassy, Phys. Rev. C **72**, 034907 (2005).
[36] W. Busza, Acta Phys. Pol. B **35**, 2873 (2004).
[37] J. F. Gunion and G. Bertsch, Phys. Rev. D **25**, 746 (1982).
[38] U. Pettersson, ARIADNE, Lund Preprint No. LUTP 885, 1988.
[39] T. Sjostrand, Comput. Phys. Commun. **82**, 74 (1994).
[40] M. Gyulassy, P. Levai, and I. Vitev, Phys. Rev. D **66**, 014005 (2002); A. Adil, M. Gyulassy, W. A. Horowitz, and S. Wicks, Phys. Rev. C **75**, 044906 (2007); A. Adil and I. Vitev, Phys. Lett. B **649**, 139 (2007).
[41] G. Ovanesyan and I. Vitev, J. High Energy Phys. 06 (2011) 080.
[42] T. Lappi and L. McLerran, Nucl. Phys. **A772**, 200 (2006); T. Lappi, Phys. Lett. B **643**, 11 (2006).
[43] J. Noronha and A. Dumitru, Phys. Rev. D **89**, 094008 (2014).
[44] J.-W. Qiu and I. Vitev, Phys. Lett. B **632**, 507 (2006).
[45] R. B. Neufeld, I. Vitev, and B.-W. Zhang, Phys. Lett. B **704**, 590 (2011).
[46] Z.-B. Kang, I. Vitev, and H. Xing, Phys. Lett. B **718**, 482 (2012).
[47] D. Kharzeev, E. Levin, and L. McLerran, Nucl. Phys. **A748**, 627 (2005).
[48] S. J. Brodsky and J. F. Gunion, Phys. Rev. D **17**, 848 (1978).
[49] M. Gyulassy, I. Vitev, X. N. Wang, and B. W. Zhang, arXiv: nucl-th/0302077; I. Vitev, J. Phys. G **30**, S791 (2004).
[50] M. Gyulassy, P. Levai, and I. Vitev, Nucl. Phys. **B594**, 371 (2001); Phys. Rev. Lett. **85**, 5535 (2000).
[51] M. Djordjevic and M. Gyulassy, Nucl. Phys. **A733**, 265 (2004).
[52] S. Wicks, W. Horowitz, M. Djordjevic, and M. Gyulassy, Nucl. Phys. **A784**, 426 (2007).
[53] I. Vitev, Phys. Rev. C **75**, 064906 (2007).
[54] M. Gyulassy, S. K. Kauffmann, and L. W. Wilson, Phys. Rev. C **20**, 2267 (1979).
[55] N. Borghini, P. M. Dinh, and J.-Y. Ollitrault, Phys. Rev. C **63**, 054906 (2001); S. A. Voloshin, A. M. Poskanzer, A. Tang, and G. Wang, Phys. Lett. B **659**, 537 (2008).
[56] A. Bzdak, P. Bozek, and L. McLerran, Nucl. Phys. **A927**, 15 (2014).
[57] ATLAS Collaboration, Report No. ATLAS-CONF-2014-027, 2014, http://cds.cern.ch/record/1702995.
[58] A. Bilandzic, Nucl. Phys. **A904–A905**, 515c (2013); G. Aad *et al.*, Phys. Lett. B **725**, 60 (2013); S. Chatrchyan *et al.*, Phys. Lett. B **724**, 213 (2013).